TABLE S1. Individual ion currents [in pA] at various TM potentials.

	S1		S2		S3	
	I_K	I_{Cl}	I_K	I_{Cl}	I_K	I_{Cl}
n100	-118	-318	-112	-387	-166	-393
n75	-128	-254	-120	-291	-166	-323
n50	-51	-179	-29	-166	-88	-264
n25	5	-96	3	-112	-45	-104
p25	45	94	59	94	53	59
p50	67	126	115	142	83	136
p75	174	203	118	227	88	120
p100	147	382	171	251	182	342

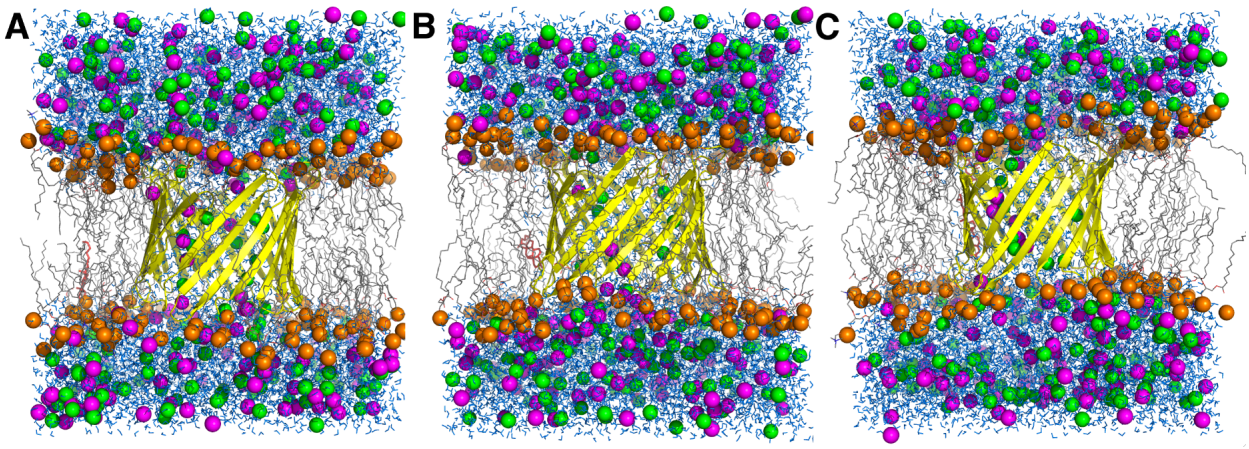

FIGURE S1. Molecular representation of systems (*A*) S1_n100, (*B*) S2_0, and (*C*) S3_p100 at the end of the simulations: hVDAC1, *yellow ribbon*; phosphates of DOPE and DOPC molecules, *orange spheres*; remainder of the lipids, *grey lines*; cholesterols, *red lines*; water, *marine*; K^+, *magenta*; and Cl^-, *green*. The figures were produced with PyMOL.

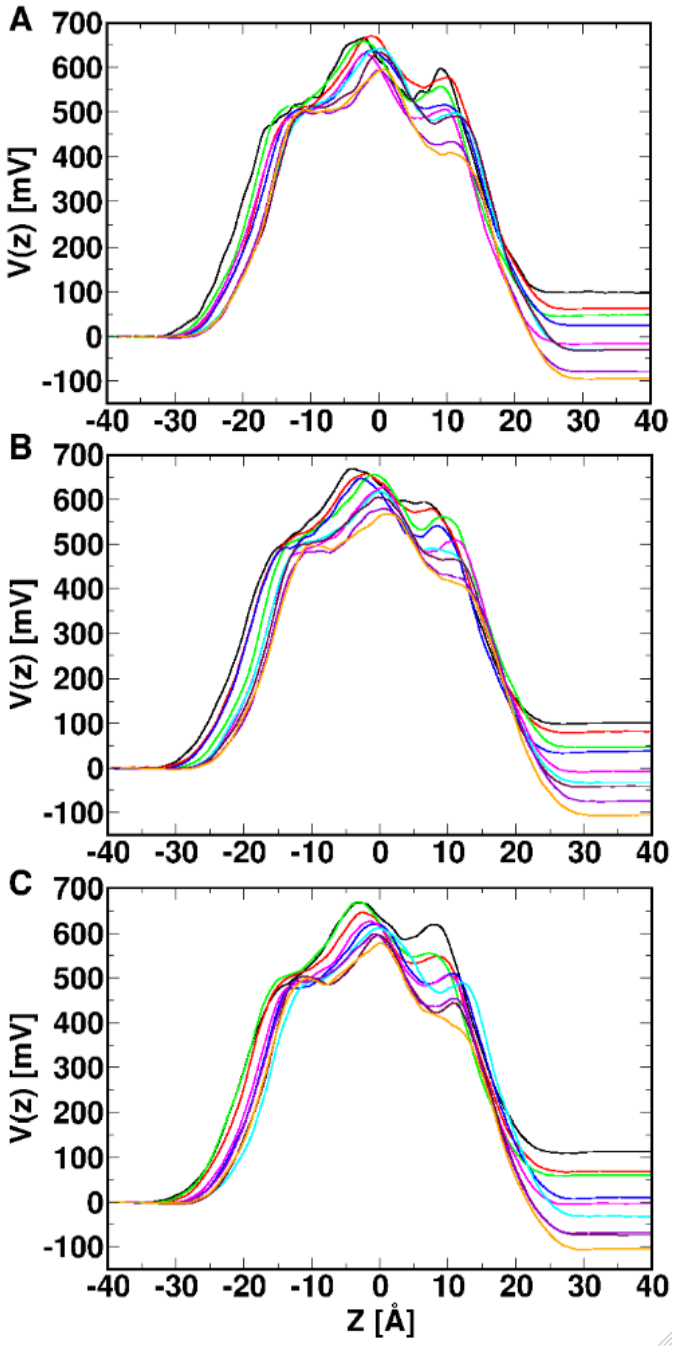

FIGURE S2. Electrostatic potential V(z) profiles along the *Z*-axis in the simulation set S1 (*A*), S2 (*B*) and S3 (*C*). Systems with different TM potentials are presented using different color schemes: V_{mp} = -100 mV (*black*), -75 mV (*red*), -50 mV (*green*), -25 mV (*blue*), 0 mV (*magenta*), 25 mV (*cyan*), 50 mV (*maroon*), 75 mV (*violet*), and 100 mV (*orange*). Because the resulting V(z) is sensitive on the choice of the integration region along the Z-axis, the calculated profiles cover different *Z*-ranges starting from *Z* = -40.0 Å to values near 40.0 Å. To clearly indicate the potential difference across the simulation cell, all the *Z*-ranges are extended to 40.0 Å with the V(z) value at their ending value between *Z* = 30.0 Å and *Z* = 35.0 Å.

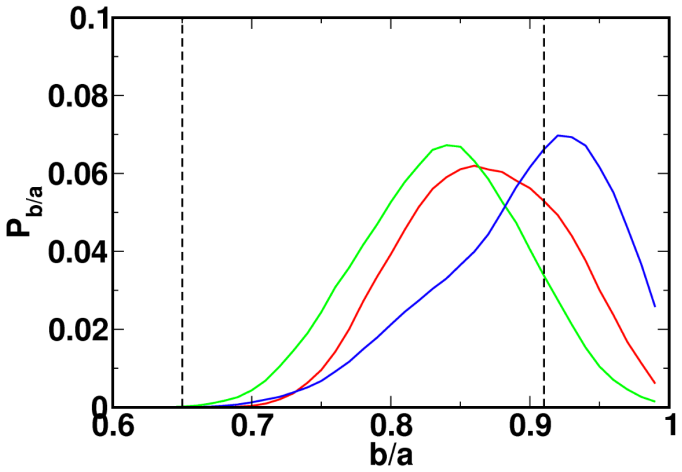

FIGURE S3. The normalized population histogram of the ratio between the short axis and the long axis of the ellipse formed by the β-barrel. The ratios are collected for systems under all TM potentials in each simulations set: S1 (*red*), S2 (*green*), and S3 (*blue*). The dashed lines show the span of the ratios calculated from the NMR structure ensemble.

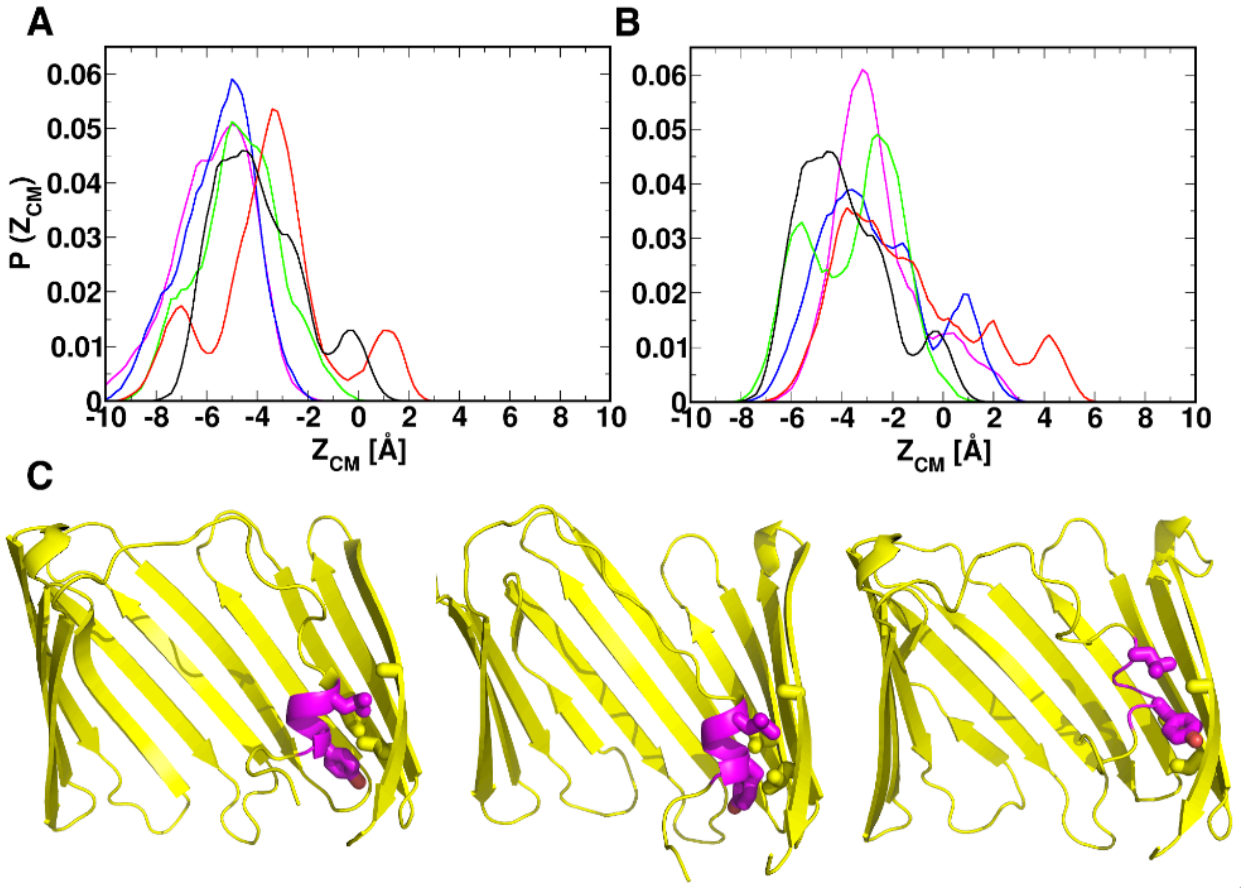

FIGURE S4. (*A* and *B*) Population of the Z-position (Z_{CM}) of the N-terminal α-helix. Z_{CM} are collected for systems with (*A*) V_{mp} = 0 mV (*black*), -25 mV (*red*), -50 mV (*green*), -75 mV (*blue*), and -100 mV (*magenta*), and (*B*) V_{mp} = 0 mV (*black*), 25 mV (*red*), 50 mV (*green*), 75 mV (*blue*), and 100 mV (*magenta*). (*C*) Interaction between the N-terminal α-helix residues (magenta sticks with Tyr7 (bottom) and Leu10 (top)) and the pore lining residues (yellow sticks with Val143 (middle), Leu150 (bottom), and Ala170 (top)): (*left*) Z_{CM} = -8.0 Å, (*middle*) Z_{CM} = -4.0 Å, and (*right*) Z_{CM} = 4.0 Å.

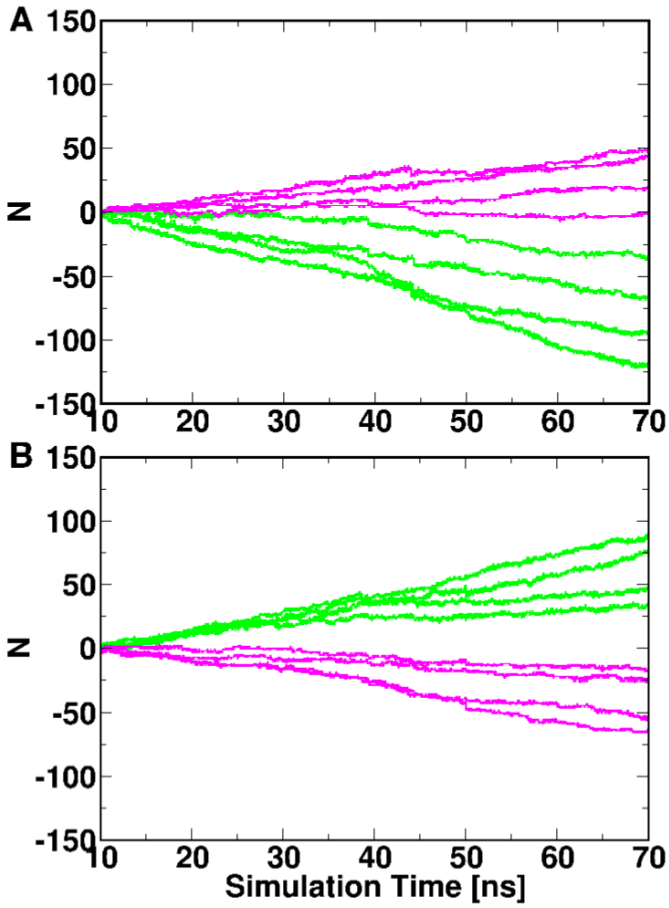

FIGURE S5. Accumulated ion crossing number for K^+ (*magenta*) and Cl^- (*green*) in the last 60 ns of the set S1 under (*A*) positive and (*B*) negative TM potentials. From top to bottom in (*A*) are V_{mp} = 100, 75, 50, 25 mV for N_K and V_{mp} = 25, 50, 75, and 100 mV for N_{Cl}. From top to bottom in (*B*) are V_{mp} = -100, -75, -50, -25 mV for N_{Cl} and V_{mp} = -25, -50, -75, and -100 mV for N_K.

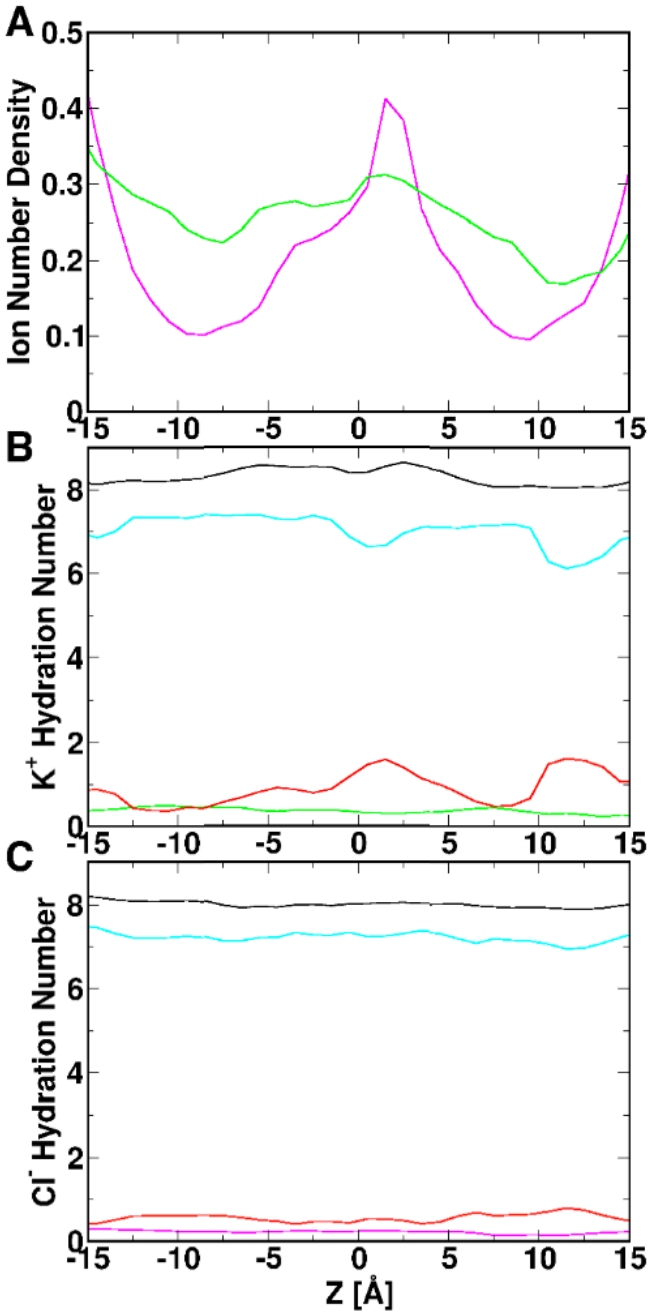

FIGURE S6. (*A*) Ion density profiles along the *Z*-axis in the pore region (-15.0 Å ≤ Z ≤ 15.0 Å): K^+ (*magenta*) and Cl^- (*green*). The densities are averaged for three independent simulations with $V_{mp} = 0$. (*B*) K^+ ion hydration number profiles and (*C*) Cl^- ion hydration number profiles along the *Z*-axis in systems with $V_{mp} = 0$. The hydration partners for K^+ include water oxygen (*cyan*), protein oxygen (*red*) and Cl^- ions (*green*), while those for Cl^- include water oxygen (*cyan*), protein nitrogen (*red*) and K^+ ions (*magenta*). The total hydration number (*black*) is also shown. A cutoff of 4.0 Å is used to count the hydration partners.

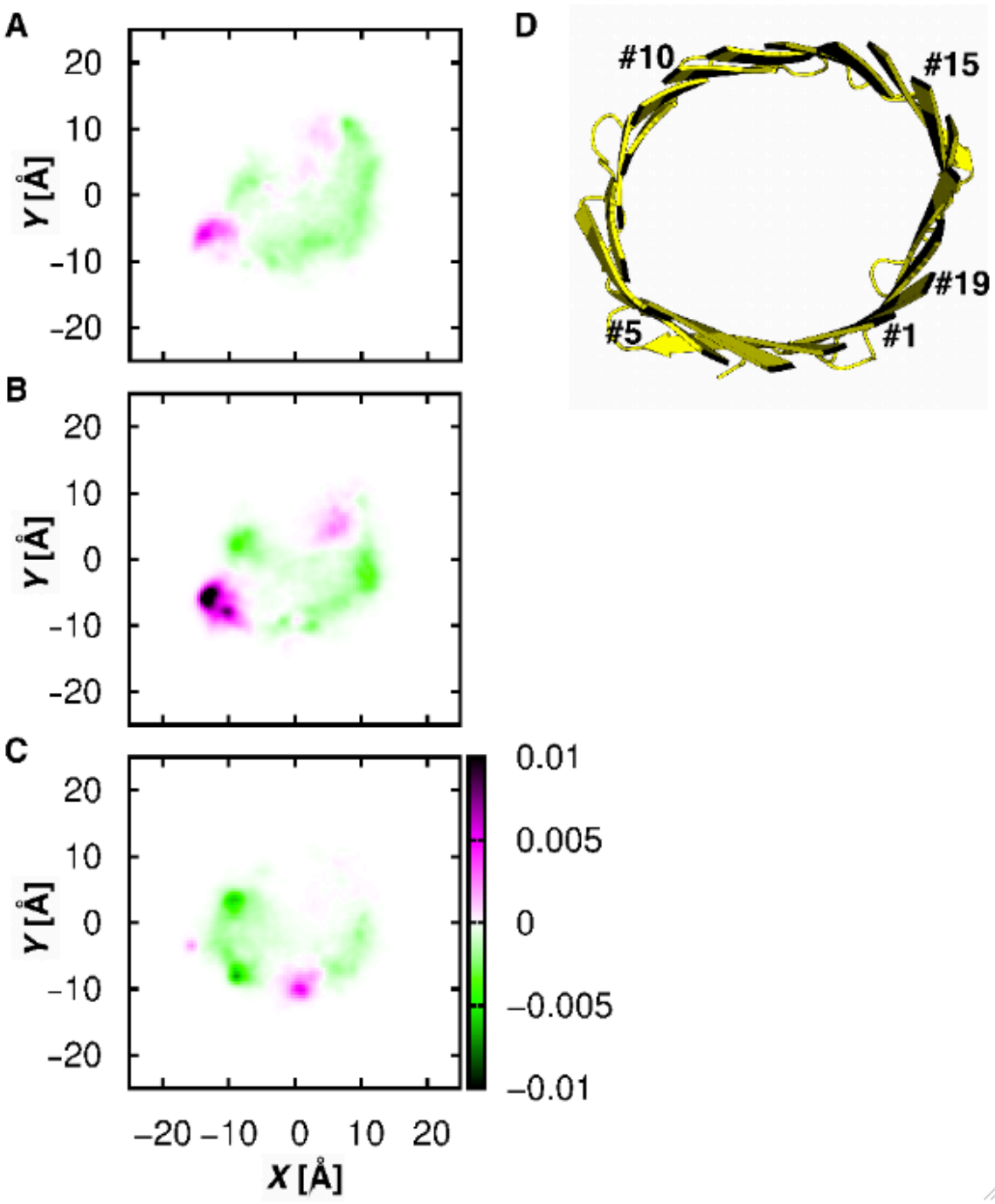

FIGURE S7. Cross-sectional ion distributions on the *X*-*Y* plane in three regions along the Z-axis: (*A*) 4.0 Å ≤ *Z* ≤ 8.0 Å, (*B*) -2.0 Å ≤ *Z* ≤ 2.0 Å, and (*C*) -8.0 Å ≤ *Z* ≤ -4.0 Å. The charge distributions are calculated from S2_0. (*D*) A molecular representation of hVDAC1 channel with its β-strands numbered. The first β-strand from the N-terminus of the channel is numbered as #1.

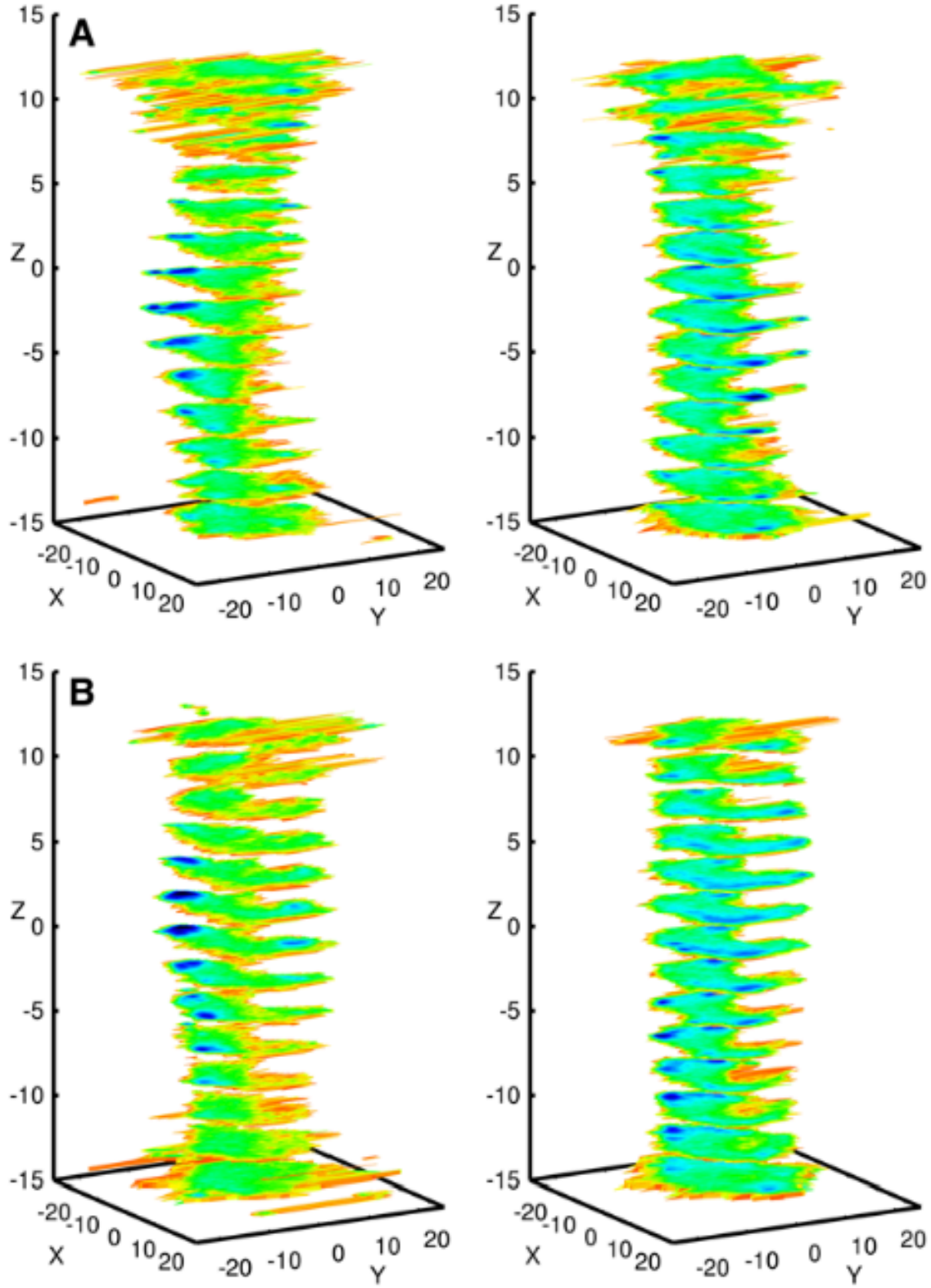
A
B
15
10
5
0
-5
-10
-15
Z
-20
-10
0
10
20
X
Y

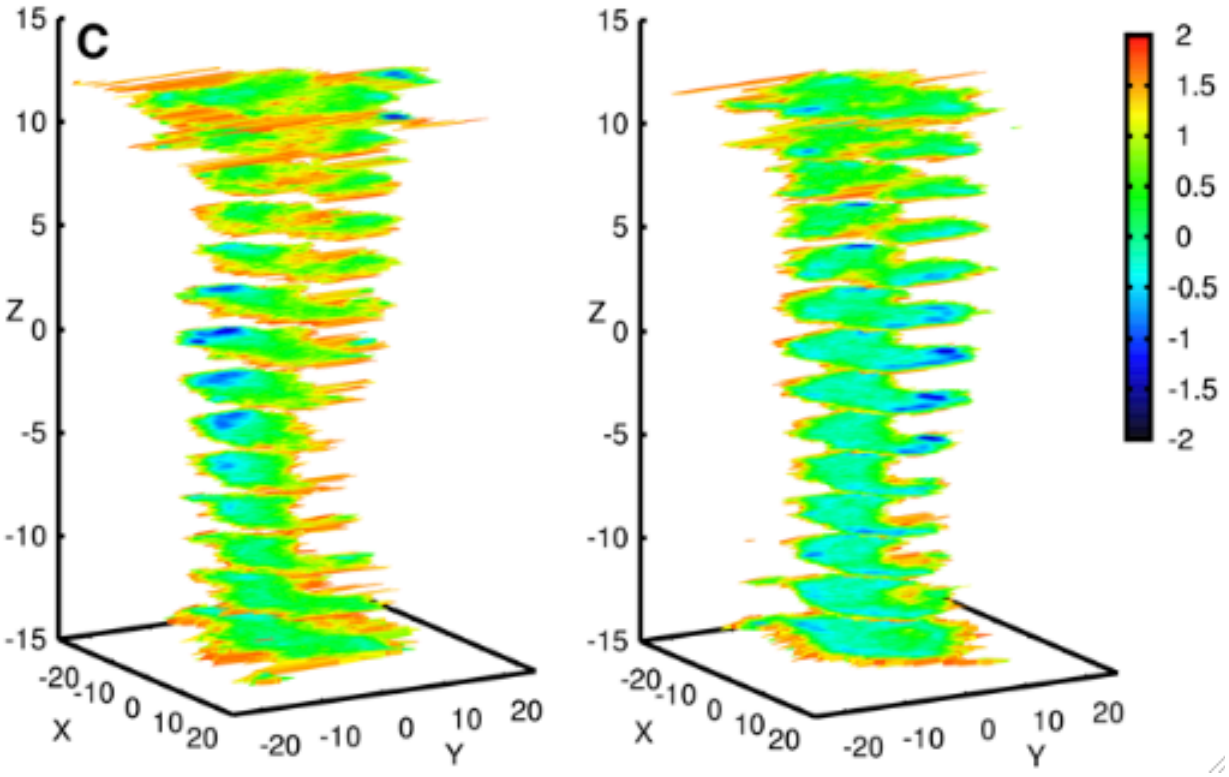

FIGURE S8. Two-dimensional multi-ion PMF profiles [in kcal/mol] for both K^+ (*left*) and Cl^- (*right*) in systems (*A*) S1_0, (*B*) S2_0, and (*C*) S3_0. The PMF profiles are calculated using $\mathcal{W}_{\alpha,\mathbf{2D}}\left(X,Y\right) = -k_{\mathbf{B}}T\,\mathbf{ln}\left[C_{\alpha}\left(X,Y\right)/C_{\mathbf{ref}}\right]$ for 2 Å slabs along the Z-axis, ranging from -14 Å to 14 Å, in which $k_{\mathbf{B}}$, $C_{\alpha}\left(X,Y\right)$, and C_{ref} are the Boltzmann constant, local ion concentration at (*X*, *Y*), and the bulk ion concentration. The PMF plots from different simulations are very similar, indicating a good convergence of ion distribution inside the pore.

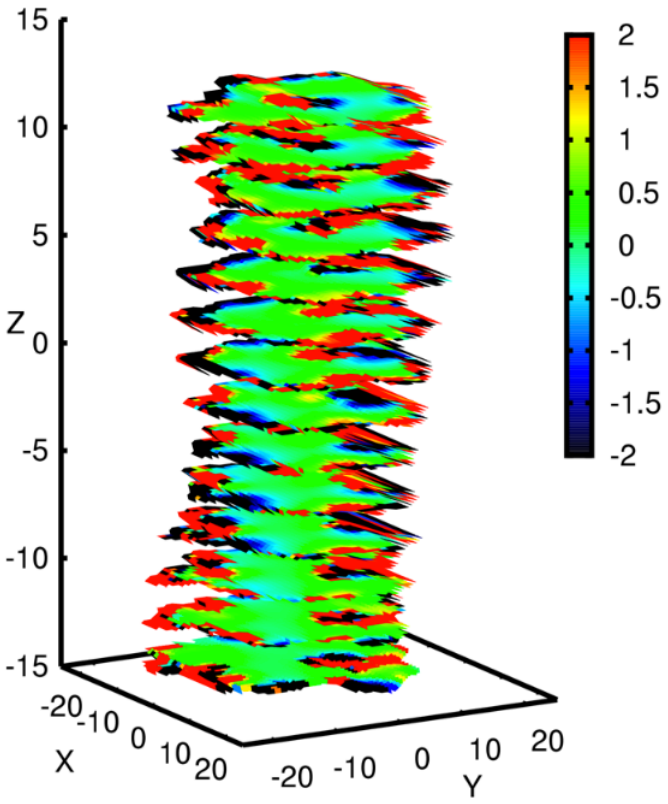

FIGURE S9. Two-dimensional electrostatic potential profile [in kcal/mol] probed by a unit charge inside the channel pore based on hVDAC1 NMR model #1. The electrostatic potential was computed using the PBEQ Solver module in CHARMM-GUI. The regions with negative electrostatic potential are favored by K^+ ions and the positive electrostatic potential regions by Cl^- ions. The electrostatic potential profiles are well correlated with the calculated two-dimensional multi-ion PMFs in Figure S8.